Macroscopic and microscopic approaches toward bacterial adhesion

Vadillo Rodríguez, Virginia

8

Role of lactobacillus cell surface hydrophobicity as probed by AFM in adhesion to surfaces at low and high ionic strength

Virginia Vadillo Rodríguez, Henk J. Busscher, Willem Norde, Joop de Vries and Henny C. van der Mei[*]

8.1 INTRODUCTION

Lactobacilli are found widely distributed throughout nature and have been used for a long time in processing and preservation of food (Holzapfel *et al.*, 1998). In addition, several studies have ascribed probiotic properties to certain lactobacillus strains, which are naturally found in the gastrointestinal or female urogenital tracts of both humans and animals (Herthelius *et al.*, 1989; Sanders, 1993). In all

[*] Submitted to *Colloids and Surfaces B: Biointerfaces*

instances mentioned, the behavior of lactic acid bacteria is dependent on interfacial processes and hence on the cell surface physico-chemical properties.

The major surface-exposed protein in many lactobacillus species is located in the S-layer. The S-layer consists of one species of (glyco-)protein, the S-protein, which is assembled into characteristic two-dimensional crystalline layers at the cell surface. This assembly is an entropy-driven process during which individual S-protein monomers form multiple interactions with each other and with the underlying cell envelope (Beveridge, 1994). Although no generalized function is known for bacterial S-layers, their presence at the outermost cell surface suggests a role in adhesion.

Bacterial adhesion to surfaces is determined by an interplay of different physico-chemical surface properties, most notably hydrophobicity and electric charge of the surfaces of the bacterial cell and the substratum. Both the hydrophobicity and the electric charge are consequences of the chemical composition of the surfaces. It is known that SLP conveys hydrophobicity to the lactobacillus cell surface (Van der Mei *et al*., 2003). Yet, adhesion of lactobacilli to surfaces often does not proceed according to expectations based on their cell surface hydrophobicity and hydrophobic strains do not always adhere best to hydrophobic substrata (Millsap *et al.*, 1996), as predicted by surface thermodynamics (Absolom *et al.*, 1983). This suggests that cell surfaces of lactobacilli may adapt their hydrophobicity in response to environmental changes, like in pH or ionic strength (Vadillo-Rodríguez *et al*. 2004).

The interaction between bacteria and solid substrata is often described by the Derjaguin-Landau-Verwey-Overbeek (DLVO) theory for colloidal stability (Dejaguin & Landau, 1941; Verwey & Overbeek, 1948). The DLVO theory can be used to calculate the Gibbs energy of interaction between surfaces as a function of their separation distance. The total Gibbs energy of interaction is interpreted as the sum of attractive Lifshitz-Van der Waals interactions and an electrostatic contribution. In general, both bacteria and substratum surfaces are negatively charged and the electrostatic contribution is repulsive as a result of their overlapping electrical double layers (Marshall, 1976). Three different situations may be distinguished, depending on the electrolyte concentration of the surrounding medium. (i) At low electrolyte concentrations, when the double layers are extensive, a large Gibbs energy barrier has to be passed to reach close contact between the two surfaces. Hence, the bacterial cell is effectively repelled from the substratum surface. (ii) At intermediate electrolyte concentration, a (shallow) secondary minimum may be formed at some separation distance (typically 5 to 20 nm), where the organism may be captured in a reversible manner and (iii) at high electrolyte concentrations, the net interaction is attractive at all separation distances and results in a strong usually irreversible adhesion. In practice, the effect of hydrophobicity and electric charge on bacterial adhesion is generally studied by quantification of the number of attached organisms on substrata with different wettabilities and from different ionic strength suspensions (Millsap *et al.*, 1996).

Experimentally, a parallel plate flow chamber is an extremely suitable device

for monitoring the initial stages of bacterial adhesion *in situ*. Accurate measurements of the kinetics of the adhesion process can be performed and modern image analysis techniques have made it possible to enumerate adhesion and desorption simultaneously during deposition (Meinders *et al*., 1992; Sjollema *et al.*, 1989). The measured desorption will therefore reflect the thermodynamic reversibility of the process, but may also include a contribution of collisions between flowing and adhering organisms as occurring in natural systems (Van de Ven, 1989).

Atomic force microscope (AFM) has emerged as a valuable tool for probing interaction forces as well as structural and physical properties of living microorganisms under physiological conditions. For instance, the role of hydrophobic interactions was pointed out by Ong *et al.* (1999) measuring the interaction forces between *Escherichia coli*-coated probes and solid substrata of different hydrophobicities. It was shown that both attractive forces and cell adhesion were promoted by the hydrophobicity of the substratum surfaces. Using nano-indentation measurements in aqueous solution, Yao *et al.* (2002) characterized the turgor pressure of several bacterial species, which were found to withstand an internal pressure of 4 to 6×10^5 Pa. It was also demonstrated in a recent paper that the elasticity of the cell wall of *Saccharomyces cerevisiae* varies significantly across the cell surface whereas a tenfold increase in Young's modulus was found for the bud scar, in agreement with the accumulation of chitin in this region of the cell wall (Touhami *et al*., 2003). In addition, several studies have shown that quantitative force measurements can be obtained by functionalizing AFM probes with self-assembled monolayers (SAMs) of organic thiols terminated with selected terminal groups. Up to date, a variety of thin organic films, polymer surfaces and fungal spores have been characterized by using AFM tips functionalized with hydrophobically and hydrophilically terminated SAMs (Vezenove *et al.*, 1997; Sinniah *et al.*, 1996; Dufrêne, 2000). Recently, information on local isoelectric points have been reported for the yeast surface *S. cerevisiae* by studying its interaction with AFM probes modified with ionizable groups (Ahimou *et al.*, 2002). Furthermore, it has been suggested that bacterial cell surface hydrophobicity or hydrophilicity can be assessed by comparison of the interaction forces between hydrophobically or hydrophilically modified AFM probes and a bacterial cell surface (Vadillo-Rodríguez *et al*., 2004).

The aim of this chapter is to investigate the role of lactobacillus cell surface hydrophobicity as probed by functionalized AFM tips, *i.e.* terminated with hydrophobic ($-CH_3$) or hydrophilic (–OH) groups, on their adhesion to surfaces from low and high ionic strength suspensions. The adhesion of *Lactobacillus acidophilus* ATCC4356 and *Lactobacillus casei* ATCC393 with and without SLP, respectively, has been measured in a parallel plate flow chamber from low and high ionic strength suspensions to similarly functionalized glass surfaces and discussed against the background of the DLVO theory and the interaction forces measured through AFM.

8.2 MATERIALS AND METHODS

8.2.1 Bacterial strains, growth conditions and harvesting

Two lactobacillus strains, *L. acidophilus* ATCC4356 and *L. casei* ATCC393 with and without S-layer respectively, were used in this study. Bacterial strains were streaked and grown for 24 h from frozen stock on MRS (De Man, Rogosa, Sharpe, Merck, Germany) agar plates and incubated at 37 ºC in an atmosphere containing 5 % CO_2. Pre-cultures were grown under the same conditions by inoculating MRS broth with a colony from the agar plate. This culture was used to inoculate a second culture that was grown for 16 h prior to harvesting. Bacteria were harvested by centrifugation (5 min at 10,000 g), washed twice with demineralized water and suspended in 10 or 100 mM KCl buffer solution.

8.2.2 Substrata and tip modification

Glass plates used in experiments were cleaned by sonicating for 2 min in 2 % RBS35 surfactant solution in water (Omnilabo International BV, The Netherlands), rinsed thoroughly with tap water, dipped in methanol, and again rinsed with demineralized water. Clean glass plates together with long/thin AFM "V"-shaped silicon nitride cantilevers from Digital Instruments Inc. (Santa Barbara, CA) were coated with electron beam thermal evaporation with a 4-nm-thick titanium layer followed by a 30-nm-thick gold layer. The coated substrata and cantilevers were immersed for 18 h in 1 mM solutions of $HS(CH_2)_{11}OH$ and $HS(CH_2)_{17}CH_3$ in ethanol and then rinsed with ethanol. Functionalized substrata and probes were always used immediately after preparation. In order to validate the quality of the surface modification, water contact angles were measured on functionalized glass surfaces. Water contact angles amounted to 10 – 20 degrees and 90 – 100 degrees for hydroxyl (–OH) and methyl ($–CH_3$) terminated surfaces, respectively.

8.2.3 Parallel plate flow chamber and data analysis

The parallel plate flow chamber (internal dimensions: 76×38×0.6 mm) and image analysis system have been described in detail previously (Busscher & Van der Mei, 1995). Images were taken from the bottom functionalized glass plate (55×38 mm) of the parallel plate flow chamber. The top plate of the chamber was made of glass and it was cleaned as described above. The flow chamber was cleaned with Extran (Merck, Germany) and thoroughly rinsed with water and demineralized water. Prior to each experiment, all tubes and the flow chamber were filled with 10 mM or 100 mM KCl solution, taking care to remove all air bubbles from the system. Once the system was filled, a bacterial suspension of 7.5×10^7 cells ml^{-1} in 10 mM or 100 mM KCl was allowed to flow through the system at a flow rate of 1.44 ml min^{-1}, corresponding with a Reynolds number of 0.6 and a wall shear rate of 10.6 s^{-1}. Deposition was observed with a CCD-MXRi camera (High technology) mounted on a phase-contrast microscope (Olympus BH-2) equipped with a 40x ultra-long-working distance lens (Olympus ULWD-CD Plan 40 PL). The camera was coupled to an image analyser (TEA; Difa). The bacterial suspension was perfused through the system for 4 h with re-circulation at room temperature.

The total number of adhering bacteria per unit area $n(t)$ was recorded as a function of time by image sequence analysis during 4 h and the affinity of an organism for the glass surface was expressed as an initial deposition rate j_0, representing the initial increase of $n(t)$ with time (see Figure 8.1). Note that since the initial deposition rate is extracted only from the initial adhesion data, it represents the affinity of the organisms for the substratum surface without intervening influences of interactions between adhering bacteria. From the total number of adhering bacteria per unit area as function of time $n(t)$ and the number of particles adhering over the full duration of an experiment n_∞, the so-called characteristic adhesion time τ was calculated using

$$n(t) = n_\infty (1-e^{-t/\tau}) \tag{8.1}$$

The characteristic adhesion time τ is determined by a combination of deposition, blocking and desorption, according to

$$1/\tau = \beta + j_0 A_b \tag{8.2}$$

in which A_b represents the area on the substratum surface blocked by one adhering bacterium and β is the desorption rate coefficient (Bos *et al*., 1999). In order to obtain the two unknowns A_b and β from Eq. 2, blocked areas were derived from the radial pair distribution $g(r)$, as can be calculated from the spatial arrangement of the adhering bacteria (Sjollema & Busscher, 1990). Inserting the blocked areas A_b derived from the radial distribution functions, and the characteristic adhesion times τ from the measured kinetics, the desorption rate coefficients β can be directly calculated from Eq. 8.2.

All values given in this chapter are the average of three experiments carried out with separately grown microorganisms.

8.2.4 AFM

Sample preparation. Bacterial cells were attached through electrostatic interactions to a glass plate made positively charged through adsorption of poly-L-lysine hydrobromide. The glass plates were first cleaned as previously described, after which a drop of 0.01 % (wt/vol) poly-L-lysine hydrobromide solution was added. After air-drying, the plate was rinsed with demineralized water and dipped into a bacterial suspension of concentration 10^5 per ml. After 15 min, the bacteria-coated glass was rinsed to remove loosely attached bacteria and transferred to the AFM.

AFM measurements. AFM measurements were made at room temperature under 10 and 100 mM KCl solution using an optical level microscope (Nanoscope III Digital Instrument). An array of 32×32 force-distances curves with z-displacements of 100 – 200 nm at z-scan rates ≅10 Hz were collected over the entire field of view when a bacterium was imaged (see Figure 8.2a and 8.2a' as an example). The slopes of the retraction force curves in the region where probe and sample are in contact were used to convert the voltage into cantilever deflection. The conversion of deflection into force was carried out as has been previously described by others (Dufrêne *et*

a)

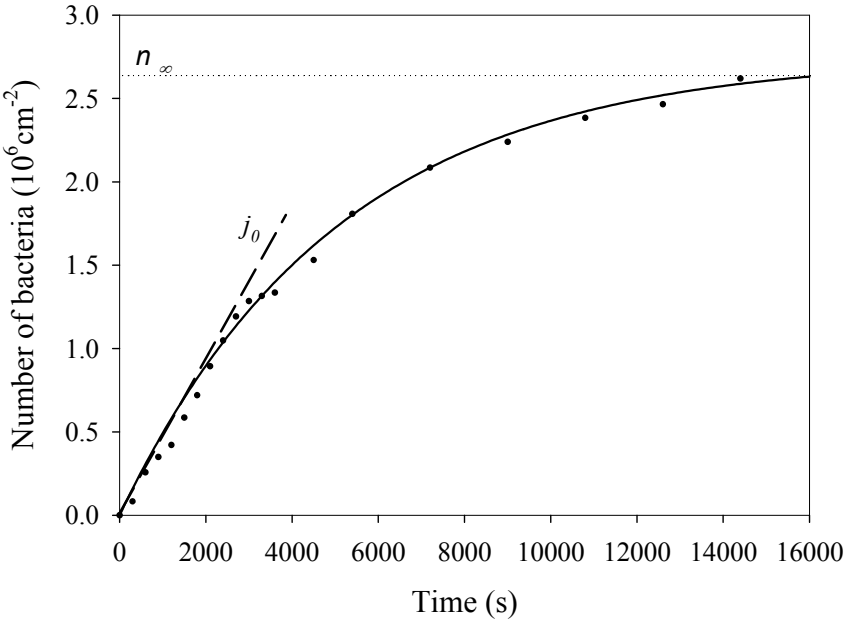

b)

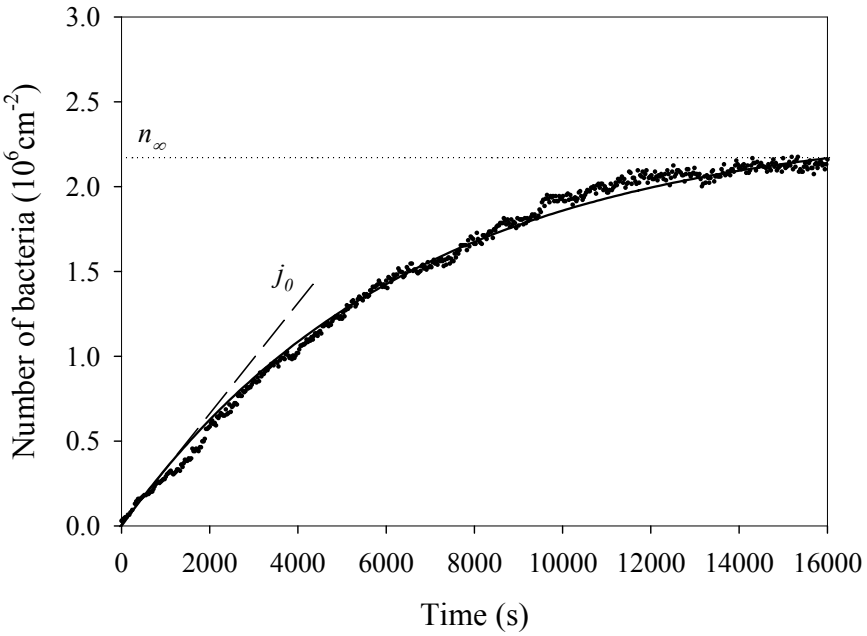

Figure 8.1 Number of bacteria deposited on hydrophilically functionalized glass as a function of time as determined in the parallel plate flow chamber for *L. acidophilus* ATCC4356 (with SLP) (a) and *L. casei* ATCC393 (no SLP) (b) in 10 mM KCl solution.

al., 2001) using a nominal spring constant for the functionalized tips of 0.21 N m^{-1}, as determined by the Cleveland method (Cleveland *et al.*, 1993). Force-distance curves taken over the top of each bacterium studied (see Figure 8.3 as an example) were analyzed in order to determine various characteristic parameters. Approach curves were fitted to an exponential function, where the interaction force F is described as $F=F_0 \exp(-d/\lambda)$, in which F_0 is the force at zero separation between the interacting surfaces, d the separation distance and λ the decay length of the interaction force F. The retracting curves were used to generate adhesion maps. Adhesion maps were produced by taking the most negative force detected during the retraction curve (Figure 8.3) as the value for adhesion and by plotting that value against *x-y* position of each force-distance curves (Figure 8.2b and 8.2b'). From the adhesion maps a selected area of ~800×800 nm^2 over the top of each bacterium was used to generate an adhesion distribution histogram (Figure 8.2c and 8.2c') from which an average adhesion force F_{adh} was calculated between functionalized AFM tips and the bacterial cell surface for each experimental condition studied. Three to five different organisms were studied for each particular case.

8.2.5 DLVO theory

The Gibbs energy of interaction $G(h)$ between the bacterial surfaces and the functionalized glass substrata were calculated according to DLVO theory for colloidal stability using a sphere-plane geometry. Mathematical expressions quantifying the Lifshitz-Van der Waals and electrostatic interactions can be found elsewhere (Norde & Lyklema, 1989). A Hamaker constant of 6×10^{-21} J was used, consistent with earlier work on the interaction between lactobacilli and glass across water (Boonaert *et al.*, 2001). Zeta potentials of functionalized glass were calculated from measured streaming potentials in a home-made parallel plate flow chamber (Van Wagenen & Andrade, 1980) yielding values of -29 mV and -24 mV for substrata terminated with $-CH_3$ groups and -78 mV and -64 mV for substrata terminated with –OH groups, in 10 mM and 100 mM KCl solutions, respectively (original experimental values for the streaming potential of hydroxyl terminated substrata were re-calculated to account for the conductivity contribution of the underlying gold film based on Schweiss *et al*., 2001). Bacterial zeta potentials at low and high ionic strengths were derived from measured bacterial electrophoretic mobilities at 25 °C with a Lazer Zee Meter (PenKem, Bedford Hills, NY, USA) equipped with an image analysis option for tracking and zeta sizing using the Smoluchowski theory (Wit *et al.*, 1997). The bacterial zeta potentials were -14 mV and -5 mV for *L. acidophilus* ATCC4356 and -7 mV and -2 mV for *L. casei* ATCC393, in 10 mM and 100 mM KCl solutions, respectively.

8.3 RESULTS

Figure 8.1 shows the initial deposition rate of *L. acidophilus* ATCC4356 (a) and *L. casei* ATCC393 (b) on hydrophilically functionalized glass at 10 mM. The deposition behavior of both lactobacilli at all conditions studied followed an exponential rise in time to a maximum value n_∞, of which the linear part allowed

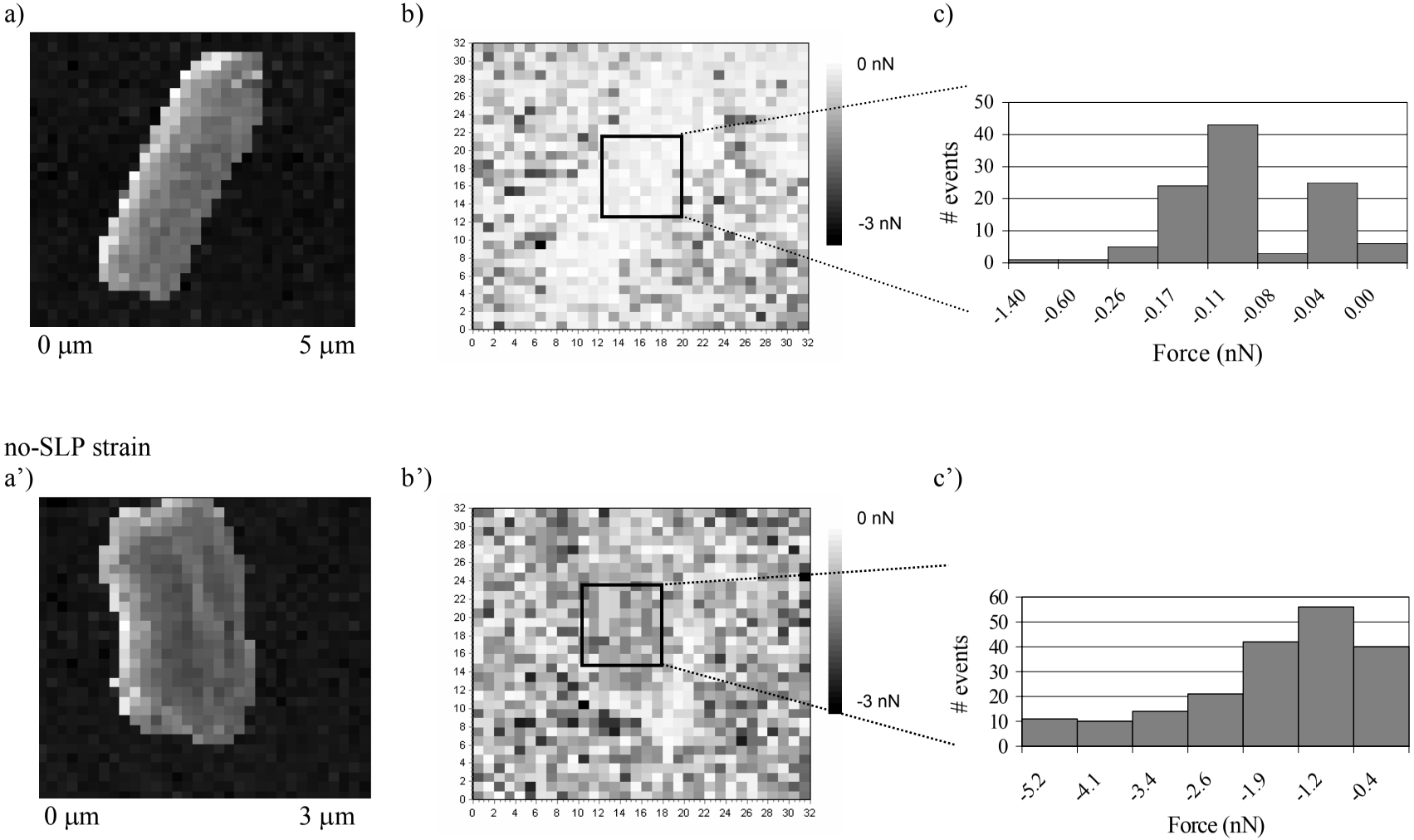

Figure 8.2 Array of 32×32 force distance curves over the AFM field of view for *L. acidophilus* ATCC4356 (with SLP) (a) and *L. casei* ATCC393 (no SLP) (a') together with their corresponding adhesion maps (b and b') obtained using a hydrophilic AFM tip in 10 mM KCl. Histograms (c and c') show the distribution of adhesion forces over a selected area of about 800×800 nm^2 on the bacterial cell surface.

a)

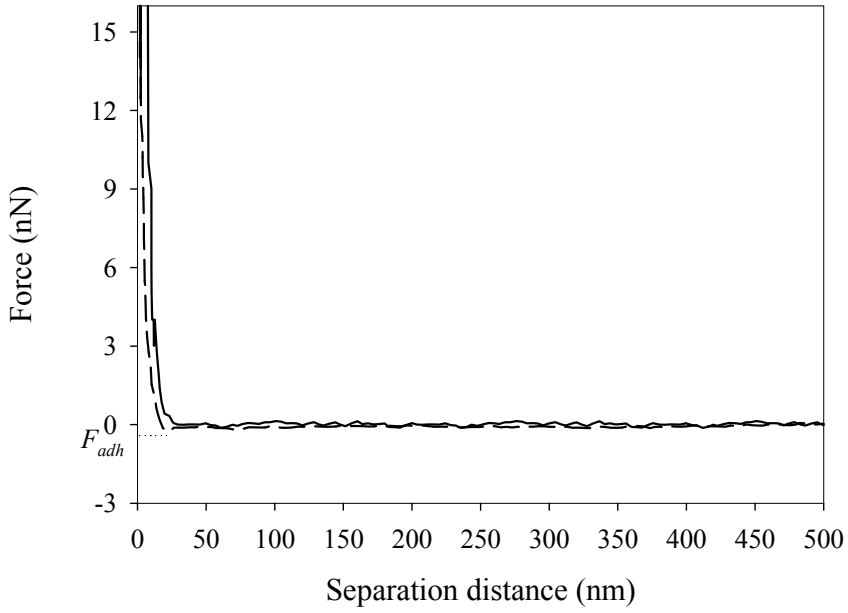

b)

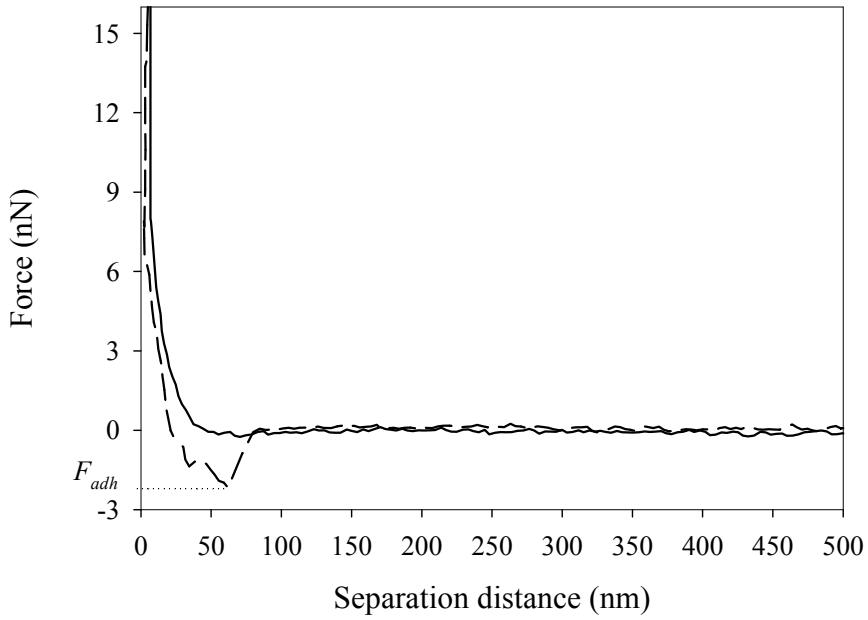

Figure 8.3. Example of force-distance curves for *L. acidophilus* ATCC4356 (with SLP) (a) and *L. casei* ATCC393 (no SLP) (b) interacting with a hydrophilic AFM tip in 10 mM KCl. The maximum adhesion force F_{adh} probed upon retraction is indicated in the graph.

a)

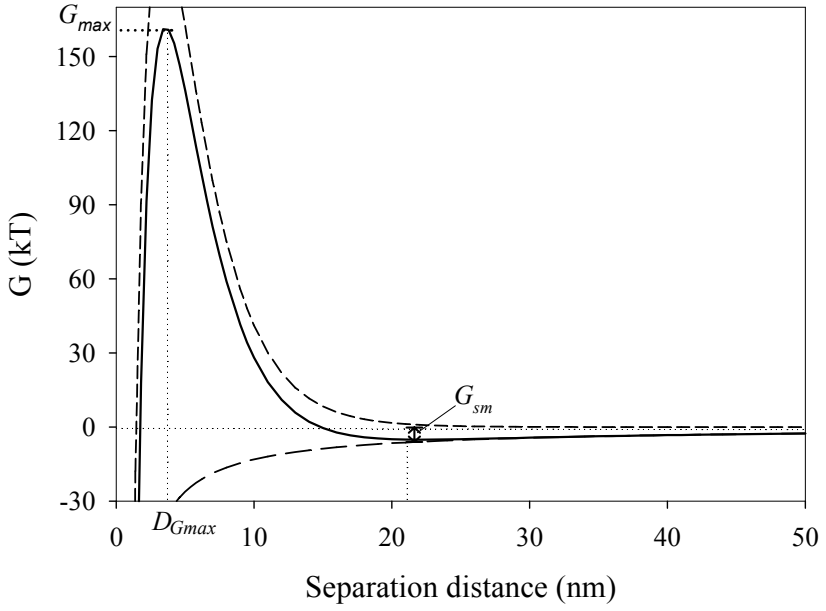

b)

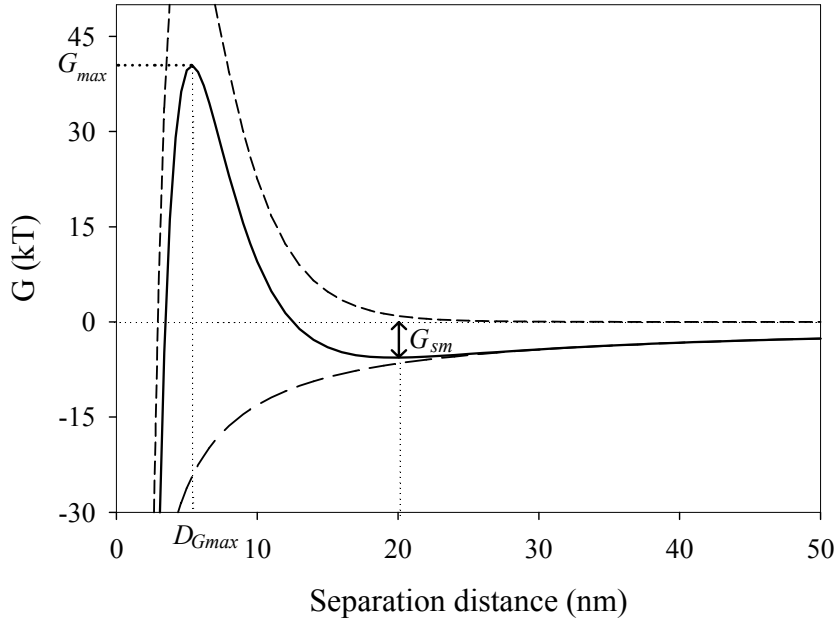

Figure 8.4. Gibbs energy curves as estimated based on the DLVO theory for colloidal stability for *L. acidophilus* ATCC4356 (with SLP) (a) and *L. casei* ATCC393 (no SLP) (b) strains interacting with hydrophilically functionalized glass in 10 mM KCl.

calculation of the initial deposition rate j_0. The initial deposition rates together with the blocked areas as calculated from the radial pair distribution function (data not shown) were used to estimate the desorption rate coefficients β. The results of the flow experiments are summarized in Table 8.1. Generally, both lactobacilli show similar adhesion patterns at the two ionic strengths. At closer look, their initial deposition rate is observed to be lower when adhering to hydrophilically functionalized glass at 10 mM. The total number of adhering bacteria after 4 h of flow n_∞ ranges from 2.2×10^6 to 6.0×10^6 cm^{-2} between the conditions studied and tends to be higher at elevated high ionic strength. The desorption rate coefficients β were only calculated for the strain lacking the SLP. Their values are small, albeit for the hydrophilic surface significantly higher than for the hydrophobic surface.

Figure 8.3 presents two examples of interactions forces measured between the strain possessing (a) and lacking (b) SLP and a hydrophilically functionalized AFM tip at 10 mM. The approach curve shows for both strains and all experimental conditions, a gradually increasing repulsion between the tip and the cell surface that increases exponentially at close approach until contact. Repulsive forces F_0 at contact as well as the force decay lengths λ are summarized in Table 8.1 as calculated over a selected area of about 800×800 nm^2 over the top of each bacterium studied. Interestingly, the strain with SLP tends to present higher values for both F_0 and λ than the strain lacking SLP. Retraction of functionalized AFM tips from the bacterial surfaces always shows a local maximum in attractive adhesion force F_{adh} (Figure 8.3). Adhesion maps show a heterogeneous surface distribution of these adhesion forces for both strains regardless of ionic strength (see Figure 8.2b and 8.2b'). The interaction forces detected were averaged per strain into an adhesion force F_{adh} based on the histograms showing their surface distribution (see Figure 8.2c and 8.2c'). Values obtained for F_{adh} are presented in Table 8.1. As a general rule, adhesion forces F_{adh} are stronger for the combination of a hydrophobic bacterium/hydrophobic tip and a hydrophilic bacterium/hydrophilic tip regardless of ionic strength.

In order to compare our results with expectations based on the DLVO theory, the total interaction Gibbs energy as a function of the separation distance was plotted for all the bacterium/substratum combinations at the two ionic strengths investigated (see Figure 8.4a and 8.4b as example). At 10 mM, for all combinations, the energy curve shows a shallow, secondary interaction minimum at separation distances between the bacteria and a substratum of 15 to 21 nm (see Table 8.1 summarizing some characteristics of the Gibbs energy curves obtained). The depth of these secondary minima varies between -5 and -7 kT, yielding for each bacterial strain the least negative values when interacting with hydrophilic substrata. The interaction Gibbs energy shows a barrier ranging between 18 kT and 161 kT at separation distance varying between 2 – 5 nm. At 100 mM the net interaction is attractive at all separation distances and for all the combinations studied. Nevertheless, bacterial desorption is still observed at conditions of 100 mM ionic strength.

Table 8.1 Summary of quantitative data describing adhesion of a lactobacillus strain with or without SLP to hydrophobic and hydrophilic substrata at low and high ionic strength, including the initial deposition rate j_0, total number of bacteria adhering after 4 h, n_∞, desorption rate coefficients β, force at zero separation distance F_0, decay length of the force λ (both from approach lines of AFM force-distance curves), and adhesion forces F_{adh} (from retraction lines). In addition, the Gibbs energy G_{sm} and location D_{sm} of the secondary minimum are given together with the position D_{Gmax} and the magnitude G_{max} of the Gibbs energy barrier. A Hamaker constant of 6×10^{-21} J and a cell radius of 1700 nm were used for the Gibbs energy calculations.

	L. acidophilus ATCC4356 Strain with SLP		*L. casei* ATCC393 Strain without SLP	
	Ionic strength		Ionic strength	
	10 mM	100 mM	10 mM	100 mM
Parallel Plate flow chamber				
$j_{0,\ phobic}$ ($cm^{-2}s^{-1}$)	571 ± 61	350 ± 59	433 ± 110	402 ± 37
$j_{0,\ philic}$ ($cm^{-2}s^{-1}$)	454 ± 22	532 ± 186	233 ± 68	427 ± 59
$n_{\infty,\ phobic}$ (10^6)	4.0 ± 0.5	4.7 ± 0.5	4.0 ± 2.0	6.0 ± 0.2
$n_{\infty,\ philic}$ (10^6)	2.9 ± 0.2	5.0 ± 0.6	2.2 ± 1.0	5.1 ± 0.6
$\beta_{,\ phobic}$ ($10^{-5}s^{-1}$)	-[a]	-[a]	7 ± 2	8 ± 1
$\beta_{,\ philic}$ ($10^{-5}s^{-1}$)	-[a]	-[a]	12 ± 2	11 ± 3
AFM				
$F_{0,\ phobic}$ (nN)	24 ± 7	22 ± 8	14 ± 2	15 ± 1
$F_{0,\ philic}$ (nN)	29 ± 7	22 ± 1	15 ± 1	15 ± 3
$\lambda_{,\ phobic}$ (nm)	30 ± 10	34 ± 12	10 ± 1	11 ± 1
$\lambda_{,\ philic}$ (nm)	12 ± 2	18 ± 2	14 ± 1	9 ± 2
$F_{adh,\ phobic}$ (nN)	-1.3 ± 0.2	-0.9 ± 0.1	-0.9 ± 0.1	-2.3 ± 0.5
$F_{adh,\ philic}$ (nN)	-0.11 ± 0.02	-2.1 ± 0.2	-2.0 ± 0.3	-0.5 ± 0.1
DLVO				
$G_{sm,\ phobic}$ (kT)	-6	-[b]	-7	-[b]
$G_{sm,\ philic}$ (kT)	-5	-[b]	-5.5	-[b]
		-[b]		-[b]
$D_{sm,\ phobic}$ (nm)	18	-[b]	15	-[b]
$D_{sm,\ philic}$ (nm)	21	-[b]	20	-[b]
		-[b]		-[b]
$G_{max,\ phobic}$ (kT)	95	-[b]	18	-[b]
$G_{max,\ philic}$ (kT)	161	-[b]	40	-[b]
		-[b]		-[b]
$D_{Gmax,\ phobic}$ (kT)	2	-[b]	3.4	-[b]
$D_{Gmax,\ philic}$ (kT)	3.4	-[b]	5.4	-[b]

[a] desorption rate coefficients β could not be estimated for these strains due to their long rod-shape, impeding calculation of the area blocked by an adhering organisms

[b] at 100 mM the total Gibbs energy curve is attractive at all separation distance regardless of the strain considered

8.4 DISCUSSION

The mechanism by which lactobacilli exert their protective functions in the intestinal and urogenital tract (Holzapfel *et al.*, 1998; Herthelius *et al.*, 1989; Sanders, 1993) is not yet known, but in order to offer their protection in a specific habitat it is essential that lactobacilli adhere well to surfaces. The presence of a regularly ordered, planar array of proteinaceous subunits (S-layer) at the outermost surface of some lactobacillus strains implies a likely role of S-layers in adhesion. S-layers of *Lactobacillus* subsp., for instance, have been shown to interact with receptors on host epithelial cells, thereby blocking receptor sites on the mucosal surfaces for the adherence of pathogenic species (Borinski & Holt, 1990).

It has been known that S-layers convey hydrophobicity to the lactobacilli cell surface. However, it was pointed out that strains with an SLP do not necessarily adhere better to hydrophobic substrata than strains without SLP (Van der Mei *et al*., 2003) and a reversal of the cell surface hydrophobicity was recorded for both *L. acidophilus* ATCC4356 and *L. casei* ATCC393 upon increasing the ionic strength. The lactobacillus strain with SLP was found hydrophobic in 10 mM and became more hydrophilic in 100 mM, while the strain without SLP was hydrophilic in 10 mM and became hydrophobic in 100 mM (Vadillo-Rodríguez *et al*., 2004). In a recent paper (Machado *et al*., 2004), it was observed that cultures of the strain *L. casei* ATCC393 grown under hyperosmotic conditions showed a significantly higher hydrophobicity than control cultures, which in turn, were rather hydrophilic. It was suggested that H3DG and AcylH3DG glycolipids present in the membrane envelope are related to the increased cell surface hydrophobicity induced by the external ionic strength of the medium. In addition, some *L. acidophilus* species have been reported as well to be sensitive to ionic strength upon changes in the permeability properties of the cell membrane, and hence, with a probable impact on the physico-chemical properties of the bacterial cell surfaces (Fernandez Murga *et al.*, 1999). Therefore, these studies suggest that lactobacilli cell surfaces may adapt their cell surface hydrophobicity in response to environmental changes with a likely potential effect on their adhesion behavior.

In this study it is observed that the ability of *L. acidophilus* ATCC4356 and *L. casei* ATCC393 with and without SLP respectively, to adhere to hydrophobic and hydrophilic substrata is similar in low or high ionic strength media. Yet, at 10 mM ionic strength both strains showed lower initial deposition rates onto hydrophilic substrata. Considering that, according to DLVO theory, energy barriers as high as 161 kT up to 40 kT need to be overcome for *L. acidophilus* ATCC4356 and *L. casei* ATCC393, respectively in order to adhere in the primary minimum, it is very likely under those conditions the bacteria deposit in the secondary interaction minimum of the energy curve. The higher initial deposition rate found between these bacteria and the hydrophobic substratum at 10 mM could therefore be explained based on the deeper secondary minima (see Table 8.1). As well, the desorption rate coefficient β measured for the non-SLP strain is lower for the hydrophobic substratum than hydrophilic ones.

At 100 mM the DLVO theory predicts a net attractive force at all separation distances for all bacterium/substratum combinations studied. Therefore, primary minimum interaction between bacteria and substrata is expected. The data in Table 8.1 reveal that saturation values n_∞ are indeed slightly higher at 100 mM. Moreover, the mass transport in the parallel plate flow chamber can be calculated by solving the convective-diffusion equation, which describes mass transport in terms of convection, diffusion and the interaction forces operating. Solving the convective-diffusion equation needs the assumption that attractive Lifshitz-Van der Waals forces between a particle and a substratum surface are counterbalanced by the hydrodynamic drag that a particle experiences when approaching a substratum surface, while electrostatic interactions are neglected (Bos *et al*., 1999). Accordingly, a theoretical deposition rate of 566 cm^{-2} s^{-1} was found for our lactobacillus strains assuming a bacterial hydrodynamic radius of 1700 nm. Considering that the strains studied are not spherical but rod-shaped bacteria, the actual theoretical deposition rate may slightly deviate from the value calculated. It seems that the deposition efficiency *i.e.* the probability that arrival of a bacterium to a substratum will actually result in deposition, is close to unity for nearly all combinations. Hence essentially all bacteria arriving at a substratum surface will deposit either in the secondary minimum (low ionic strength) or primary minimum (high ionic strength). It would be expected that bacteria have more difficulty to desorb from the primary minimum than from the secondary minimum. However, this expectation is not corroborated by the values obtained or the desorption probabilities β. Possibly, the desorption does not reflect thermodynamic stability but is primarily determined by collisions between flowing and adhering bacteria. It is also possible that the DLVO theory, as it does not take into account short range interactions, is not applicable to predict the interaction at short separation (< 1nm).

Furthermore, it is observed that the magnitude of the forces detected upon approach of functionalized AFM tips to the bacterial cell surfaces as well as the distances over which such forces extend are not consistent with the DLVO model. AFM recorded a repulsive force F_0 regardless of ionic strength. In AFM, the contact between the surfaces interacting is imposed and it is likely that they interact in the primary minimum. At low ionic strength a repulsive force between the bacterial cell surfaces and the AFM tips was expected. The total force needed for an organism to overcome the energy barriers predicted by DLVO at 10 mM can be calculated to amount to 10^{-11} N for both lactobacillus strains. This force is three orders of magnitude lower than the force recorded by AFM. In addition, the decay lengths associated to AFM forces extend over much larger distances than theoretically predicted. Therefore, it seems that AFM fails to detect DLVO forces. Note that the total force needed for the AFM to overcome in order to reach close contact with the bacterial cell surfaces is always larger for the strain with SLP than the strain without SLP. These observations lead to the hypothesis that the AFM tips likely probe mechanical cell surface properties upon approach, including electrosteric repulsions in addition to interaction forces. Consequently, the results obtained would reveal a harder coat for the strain having SLP, in agreement with

the proteinaceous crystalline structure known to be present at the outermost surface of these strains.

Upon retraction from the bacterial cell surfaces, the average adhesion force detected by the AFM tips is stronger for the combinations of hydrophobic bacterium/hydrophobic substratum and hydrophilic bacterium/hydrophilic substratum than for the hydrophobic/hydrophilic combinations. These adhesion strengths are not reflected in the macroscopic adhesion data (*e.g.* the desorption probability) neither at low nor high ionic strength. It is likely that the force applied when a bacterium comes into contact with a substratum as occurs in the AFM experiments influences its adhesion.

In summary, it is concluded that both *L. acidophilus* ATCC4356 and *L. casei* ATCC393 with and without SLP showed higher initial deposition rate to hydrophobic substrata at low ionic strength. At high ionic strength, a reversal of the cell surface hydrophobicity has been detected for both strains using functionalized AFM tips and no preferential macroscopic adhesion is recorded to either hydrophobic or hydrophilic substrata. This observation agrees with previous results on the adhesion of some lactobacillus strains which indicated that strains possessing a SLP do not always adhere better through hydrophobic interactions to hexadecane than strains without SLP (Van der Mei *et al.*, 2003). Boonaert *et al*. (2001) experienced as well that, in water, the adhesion behavior of another hydrophilic no-SLP lactobacillus strain could not be explained based on the cell surface hydrophobicity, since bacteria adhered in higher numbers to hydrophobic polystyrene than to hydrophilic glass. In addition, AFM measurements failed to detect DLVO forces upon approach of the functionalized tips to the bacterial cell surfaces. Upon their retraction, stronger average adhesion forces were found for the combination hydrophobic bacterium/hydrophobic substratum and hydrophilic bacterium/hydrophilic substratum, independent of ionic strength. These strong adhesion forces are not reflected in the macroscopic observations on bacterial adhesion which suggest that the force applied when a bacterium comes into contact with a substratum influences its adhesion mode.